Microsystem Technologies
https://doi.org/10.1007/s00542-020-04971-x

TECHNICAL PAPER

Thermal convective conditions on MHD radiated flow with suspended hybrid nanoparticles

C. S. K. Raju[1] · S. Mamatha Upadhya[2] · Dinesh Seth[3]

Received: 3 July 2020 / Accepted: 20 July 2020

Abstract

Adding variety of nanoparticles to the base fluid is current technique in order to boost the thermal performance of conventional fluids and mononanofluids. The forthright intention of the present investigation is to analyze numerically the up-to-date progress in flow and heat transport nature of magnetohydrodynamic, radiative Newtonian fluid, water-based Al_2O_3 nanofluid, water-based graphene nanofluid and water based Al_2O_3 + graphene hybrid nanofluid due to convectively heated stretching sheet. The flow equations are transformed by applying appropriate transformations into a pair of self-similarity equations. Further similarity equivalences are numerically solved through Runge–Kutta based shooting method. Graphs and tables are structured to analyze the behavior of sundry influential variables. From this study it is found that rate of heat transfer for Graphene + water is 2.921934, $Al_2O_3 + H_2O$ + Graphene is 2.250658 and $Al_2O_3 + H_2O$ is 3.260554. From this we conclude that water based Al_2O_3 + graphene hybrid nanofluid can be opted for cooling performance. Water based Al_2O_3 nanofluid significantly enhance convection heat transfer performance over a stretching sheet. Friction at the wall for Graphene + water is (− 1.719525), $Al_2O_3 + H_2O$ + Graphene is (− 2.256614) and $Al_2O_3 + H_2O$ is (− 1.959539). From this we conclude that water based Al_2O_3 + graphene hybrid nanofluid shows lower wall friction rate compared to other two mixture compositions.

List of symbols

u_1, v_1 (ms^{-1})	Velocity components
x_1, y_1 (m)	Cartesian coordinates
T (K)	Temperature of the fluid
T_w (K)	Wall Temperature
T_∞ (K)	Ambient fluid temperature
g (ms^{-2})	Acceleration due to gravity
k (W m^{-1} K^{-1})	Thermal conductivity
p (kg m^{-1} s^{-2})	Pressure
μ (kg m^{-1} s^{-1})	Dynamic viscosity
υ(m^2 s^{-1})	Kinematic viscosity
ρ(kg m^{-3})	Fluid density
c_p(J kg^{-1} K^{-1})	Specific heat capacity at constant pressure
σ^* (W m K^{-4})	Stefan–Boltzmann constant
τ_w(kg m^{-1} s^{-2})	Wall shear stress
k^*	Mean absorption coefficient
M	Magnetic parameter
Bi	Biot number
σ(kg^{-1} m^3 A^2)	Electrical conductivity
ϕ	Nano particle volume fraction
Pr	Prandtl number
R	Radiation parameter
ζ	Similarity variable
C_f	Skin friction coefficient
Nu_x	Local Nusselt number
Re	Local Reynolds number

Subscripts

∞	Ambient condition

✉ C. S. K. Raju
sivaphd90@gmail.com; rchakrav@gitam.edu

S. Mamatha Upadhya
mamathasupadhya@gmail.com

Dinesh Seth
dseth@gitam.edu

[1] Department of Mathematics, GITAM School of Science, GITAM Deemed to be University, Bengaluru-Campus, Bengaluru, Karnataka, India

[2] Department of Mathematics, Kristu Jayanti College, Autonomous, PO, K.Narayanapura, Kothanur, Bengaluru, Karnataka 560077, India

[3] Department of Mechanical Engineering, GITAM School of Technology, GITAM Deemed to be University, Bengaluru-Campus, Bangalore, Karnataka 562163, India

Published online: 31 July 2020

f	Regular fluid
nf	Single nanoparticle nanofluid
hnf	Hybrid nanofluid

1 Introduction

In the world persistently researchers are working for the development of new materials which would focus on efficient heat and mass transport system. In this regard several researchers and engineers have proved that nanofluid would enhance the thermal efficiency of the system compared with bulk materials. Nanofluids are engineered colloids consisting of nanoparticles (1–100 nm) and a base fluid. Researchers are still investigating the hidden characteristics of nanofluid. Recently, Sajid et al. (2019) experimentally investigated heat transfer nature of TiO_2 nanofluid by varying the concentrations TiO_2 nanofluid and found that TiO_2 nanofluid has better heat transport characteristics compared to distilled water. Gopal et al. (2020) studied the influence of heat generation/absorption along with thermal stratification on Carreau nanofluid over a permeable cylinder and found that in order to get more friction it is better to incorporate curvature parameter in the flow. Upadhya et al. (2020) compared heat transfer characteristics of graphene nanofluid considering two different base fluid ethylene glycol and water. They observed that ethylene glycol based graphene nanofluid shows better heat transfer compared to water based graphene nanofluid. Raju et al. (2019) explored the influence of magnesium oxide nanoparticles in nonlinear boundary layer flow and found that improvement in non linear convection parameter improves heat transfer rate. Seth et al. (2016, 2018) observed that nanofluid not only support energy efficiency but also augment green manufacturing management initiatives. Sajid and Ali (2019) analyzed that shape and size of nanoparticles has key role in the heat transfer enhancement. Abdelrazek et al. (2020) investigated heat transfer of nanofluids by considering different geometry and found that different heat transfer rate for the same nanofluid in square and circular tube flows. Chen et al. (2020) took up experimental investigation on bubble characteristics of time periodic subcooled flow boiling in annular ducts due to wall heat flux oscillation and found that bubble size reduced after time lag. Tariq et al. (2020) investigated thermal performance of normal-channel facile heat sink using water and TiO_2–H_2O nanofluids. They observed maximum reduction in base temperature for TiO_2–H_2O nanofluid. Shahsavar et al. (2020) reported that improving Re, T_{in} and amplitude of wavy wall increases the system performance during melting and solidification mechanisms. Khalid et al. (2020) has discussed in detail about various techniques applicable for improvement in thermal performance of heat types such as use of nanofluids and self- rewetting fluids, manufacturing various types of fins and grooves, inner surface treatment, use of different types of wicks, using different inclination angles in heat types.

Currently, researchers have thought about new kind of nanofluid called 'Hybrid nanofluid' which is the amalgamation of two different types of nanoparticles in the base fluid. Hybrid nanoparticle is formed by the combination of physical and chemical properties of two or more nanoparticles simultaneously to obtain a homogeneous phase. Researchers are vigorously working on heat and transport phenomena of this kind of fluid material and have demonstrated that Hybrid nanofluid has high efficient thermal conductivity, effective heat transfer, advantages of individual suspension, stability lower operating cost, better performance than the nanofluid. Application field of Hybrid nanofluids includes all the areas of heat transfer like electronic cooling, generator cooling, vehicle thermal management, coolant in machine, nuclear system cooling, thermal storage, biomedical, refrigeration, space aircrafts, heat pipe, lubrication etc. Recently, Sajid and Ali (2018) explored thermal conductivity of hybrid nanofluids and suggested that appropriate selection of hybrid nanoparticles plays a key role in attaining stability of the fluid. Babar et al. (2019) noticed that fluids comprising tube shaped nanoparticles exhibits greater viscosity compared to spherical shape nanoparticles. Muhammad et al. (2020) took up comparative study in squeezed flow of hybrid nanofluid and nanofluid and found that performance of hybrid nanofluid is effective. Sheikholeslami et al. (2019) investigated flow properties by dispersing hybrid nanoparticles into water inside a wavy tank. Kumar et al. (2020) analyzed Blasius and Rayleigh stokes on hybrid nanofluid flow and found that nanoparticles generate warmness because of the photocatalytic nature.

Considerable attention is provided today by the researchers towards aluminium oxide Al_2O_3 (alumina) nanoparticles owing to its significant increment in propellant burning rate as well as coolent, lower ignition time and temperature. Al_2O_3 is ideal material of far-infrared emission. Due to its exceptional properties aluminium nanoparticles are applicable in aerospace applications, modern solid rocket propellants normally contains aluminium powder as fuel owing to its high energy release during the oxidation process to alumina, in automobiles, corrosion, heat shielding coating of aircraft etc. In liquid form Al_2O_3 nanoparticles are used in plastics, ceramics, rubber, refractory products in order to improve ceramics density, fracture toughness, creep resistance, wear resistance, smoothness etc. The morphology of Al_2O_3

nanoparticles is spherical and would appear as white powder. Wakif et al. (2020) studied the influence of surface roughness and thermal radiation considering alumina-copper oxide hybrid nanofluid and found that improvement in roughness parameter upsurge the stability of the hybrid nanofluid. Sriharan et al. (2020) studied experimentally heat transfer performance by considering various metal oxide based nanofluids and found that Al_2O_3–DIW nanofluid has higher heat transfer coefficient.

Graphene is an atom thick honeycomb sheet of carbon atoms. In 1 mm of graphite there occur about 3 million layers of graphene. It is harder than diamond but more elastic than rubber. Its electron mobility is 100 times faster than silicon. Its electrical conductivity is 13 times better than copper. Since single layer of graphene is known for good electrical conductance and heat conductance it is used in micro and nanoelectronics. Thus, graphene could form the basis of latest carbon based microprocessor which would be more powerful than the silicon-based processors. Biomedical applications of graphene include drug delivery and medical devices. In addition, graphene is used in capacitors for energy storage, catalysts, batteries, organic light emitting diodes. Due to high mobile free π electrons graphene shows high electrical and thermal conductivity than copper. Goodarzi et al. (2019) reported that improvement in solid nano sheet volume fraction in graphene water/silver based nanofluid increased the heat transfer. Sarafraz and Safaei (2019) reported that graphene-methanol nanofluid employed inside the heat pipes could improve the thermal efficiency of the evacuated tube solar collector. Raju et al. (2019) studied unsteady nonlinear convection in Eyring Powell nanofluid and found that graphene nanofluid enhanced heat transfer performance. Sarafraz et al. (2019) indicated that application of graphene nano-platelets potentially improve the thermal conductivity of the working fluid.

The 2D flow of fluid in the vicinity of immediate of a surface is important area of research in various engineering fields such as paper production, glass blowing, drawing, continuous stretching etc. Hayat et al. (2019) studied Darcy–Forchheimer 3D rotating flow due to stretchable surface and noticed that temperature and concentration fields improved with the increase in rotational parameter. Kumar et al. (2020) studied flow of micropolar fluid past a slendering stretching surface and noticed that microrotation parameter enhance couple stress coefficient. Abd El-Aziz and Afify (2019) examined the influence of hall current and entropy on Casson fluid flow past a stretching surface. Raju et al. (2019) analyzed heat and mass transfer in Casson–Williamson fluid with non-uniform source/sink over a stretching surface. Kumar et al. (2019) analyzed that heat and mass transport process past slendering sheet match with those over a flat sheet in presence of slip flow conditions.

Considering the above mentioned applications of graphene and Al_2O_3 nanoparticles in this study we have analyzed flow and heat transport of MHD, radiative Newtonian fluid, nanofluid $((Graphene + H_2O), (Al_2O_3 + H_2O))$ and hybrid nanofluid $(\text{Graphene} + H_2O + Al_2O_3)$ over a stretching sheet considering convective boundary condition. The governing flow equations which are in PDEs are transformed into ODEs by suitable transformations. Numerically the ODEs are handled with built in Runge–Kutta based shooting method in MATLAB. Comparative studies are undertaken for velocity $f'(\zeta)$ and temperature $\theta(\zeta)$ distribution for varying parameters value for hybrid nanofluid, nanofluid and Newtonian fluid. Variation in skin friction $\left(C_f \mathrm{Re}_x^{1/2}\right)$ and local Nusselt number $\left(Nu_x \mathrm{Re}_x^{-1/2}\right)$ addressed through the preparation of graphs and tables. Further, obtained numerical results are compared with available resources.

2 Modeling of constitutive equations

Two-dimensional, incompressible flow of hybrid nanomaterial over a stretching sheet is considered. We consider Graphene and aluminium oxide (Al_2O_3) nanoparticles distributed in base fluid water (H_2O) for the present analysis. Flow is analyzed in the presence of MHD, radiation and convective boundary conditions. Cartesian coordinate frame (x_1, y_1) is considered in such a way that x_1 is extending along the convective surface and y_1 is measured normal to the surface.(u_1, v_1) are the velocity components along (x_1, y_1) axis. The flow is confined to $y_1 \geq 0$. Here, T-fluid temperature, T_f the convective surface temperature and h_f is the heat transfer coefficient. T_∞-ambient fluid temperature. B_0 is the uniform magnetic field strength which is applied in the direction transverse to the stretching surface. g is the acceleration due to gravity. Figure 1 depicts the flow problem. To attain the thermal equilibrium, Graphene/water nanofluid is constituted by dissolving a nanoparticle volume fraction ϕ_1 in water to constitute Graphene/water nanofluid. This ϕ_1 is kept constant throughout the analysis. Now, to attain our anticipated results the second nanoparticle volume fraction ϕ_2 of aluminium oxide Al_2O_3 nanoparticles is dispersed in Graphene/water nanofluid to constitute hybrid nanofluid Graphene–aluminium oxide (Al_2O_3)/water.

Following Uma Devi and Anali Devi (2017) and Manjunatha et al. (2019) the leading equations of the flow model are given by:

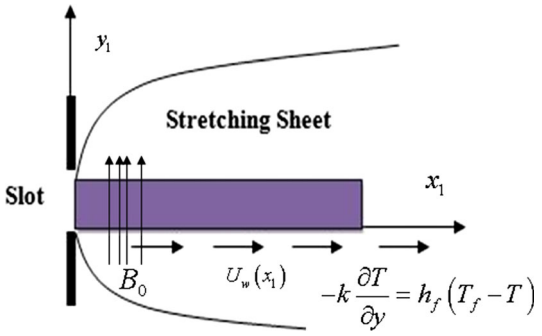

Fig. 1 Flow geometry of the problem

$$\frac{\partial u_1}{\partial x_1} + \frac{\partial v_1}{\partial y_1} = 0 \tag{1}$$

$$u_1\frac{\partial u_1}{\partial x_1} + v_1\frac{\partial u_1}{\partial y_1} = \left(\frac{\mu_{hnf}}{\rho_{nhf}}\right)\frac{\partial^2 u_1}{\partial y_1^2} - \frac{\sigma B_0^2 u_1}{\rho_{nhf}} \tag{2}$$

$$u_1\frac{\partial T}{\partial x_1} + v_1\frac{\partial T}{\partial y_1} = \left(\frac{k_{hnf}}{(\rho C_p)_{hnf}}\right)\frac{\partial^2 T}{\partial y_1^2} - \left(\frac{1}{(\rho C_p)_{hnf}}\right)\frac{\partial q_r}{\partial y_1} \tag{3}$$

The appropriate boundary conditions for the flow model are:

$$\begin{cases} v_1(x_1,0) = 0,\ u_1(x_1,0) = U_w(x_1) = cx_1,\ \ u_1(x_1,\infty) = 0, \\ -k\dfrac{\partial}{\partial y}T(x_1,0) = h_f(T_f - T),\ T(x_1,\infty) = T_\infty \end{cases} \tag{4}$$

Exploiting Rosseland approximation for radiation (following Raju et al. (2019)) the radiative heat flux (q_r) is interpreted as:

$$q_r = \left(-\left(\frac{4}{3}\right)\frac{\sigma^*}{k^*}\right)\frac{\partial T^4}{\partial y_1} \tag{5}$$

where $T^4 \approx \left(4T_\infty^3\right)T - \left(3T_\infty^4\right)$ and k^*-mean absorption coefficient, σ^* Stephen Boltzmann constant.

Considering Eq. (5) and abandoning higher order terms in $T^4 \approx \left(4T_\infty^3\right)T - \left(3T_\infty^4\right)$ (see (Hayat et al. 2019)) Eq. (3) can be reconsidered as:

$$u_1\frac{\partial T}{\partial x_1} + v_1\frac{\partial T}{\partial y_1} = \left(\frac{k_{hnf}}{(\rho C_p)_{hnf}}\right)\frac{\partial^2 T}{\partial y_1^2} + \left(\frac{16\sigma^* T_\infty^3}{3k^*(\rho C_p)_{hnf}}\right)\frac{\partial^2 T}{\partial y_1^2} \tag{6}$$

3 Similarity transformations

The requisite similarity variables (Eqs. (7)–(10)) and thermo physical properties of nanofluid and Hybrid nanofluid represented in Table 1 are considered to solve the Eqs. (1), (2), (3) and (6).

$$u_1 = cx_1\frac{df}{d\zeta} \tag{7}$$

$$v_1 = -\sqrt{(c\upsilon_f)}f(\zeta) \tag{8}$$

$$\zeta = \left(\sqrt{\frac{c}{\upsilon_f}}\right)y_1 \tag{9}$$

$$(T - T_\infty)\frac{1}{\theta(\zeta)} = (T_f - T_\infty) \tag{10}$$

Thus, following ODEs Eqs. (11) and (12) with boundary conditions, Eq. (13) are obtained.

$$\frac{d^3 f}{d\zeta^3} = \left[\left((1-\phi_1)^{(2.5)}.(1-\phi_2)^{(2.5)}\right).\left(\left(M\frac{df}{d\zeta}\right) + \left((1-\phi_2)\left[(1-\phi_1) + \phi_1\left(\frac{\rho_{s1}}{\rho_f}\right)\right] + \phi_2\left(\frac{\rho_{s2}}{\rho_f}\right)\right).\begin{bmatrix}\left(\frac{df}{d\zeta}\right)^2 \\ -f(\zeta)\frac{d^2 f}{d\zeta^2}\end{bmatrix}\right)\right] \tag{11}$$

$$\frac{d^2\theta}{d\zeta^2} = (-)\left(\frac{k_f}{k_{hnf}} + \frac{4}{3}R\right).\left((1-\phi_2)\left[(1-\phi_1) + \phi_1\left(\frac{(\rho C_p)_{s1}}{(\rho C_p)_f}\right)\right] + \phi_2\left(\frac{(\rho C_p)_{s2}}{(\rho C_p)_f}\right)\right).\left(\Pr.f(\zeta)\frac{d\theta}{d\zeta}\right) \tag{12}$$

$$f(0) = 0,\ \frac{df(0)}{d\zeta} = 1,\ \frac{d\theta(0)}{d\zeta} = -Bi(1-\theta(0)),\ \frac{df(\infty)}{d\zeta} = 0,\ \ \theta(\infty) = 0 \tag{13}$$

where $M = \left(\frac{\sigma B_0^2}{c\rho_f}\right)$ the magnetic parameter, $R = \left(\frac{4\sigma^* T_\infty^3}{k_f k^*}\right)$ the radiation parameter, $\Pr = \left(\frac{\mu_f (C_p)_f}{k_f}\right)$ the Prandtl number, $Bi = \frac{h_f}{k}\sqrt{\frac{\upsilon}{c}}$ the Biot number

Table 1 The thermo physical properties of nanofluid and Hybrid nanofluid

Properties	Hybrid Nanofluid	Nanofluid
Thermal conductivity	$\frac{k_{hnf}}{k_{bf}} = \frac{k_{s2}+(n-1)k_{bf}-(n-1)\phi_2(k_{bf}-k_{s2})}{k_{s2}+(n-1)k_{bf}+\phi_2(k_{bf}-k_{s2})}$ where $\frac{k_{bf}}{k_f} = \frac{k_{s1}+(n-1)k_f-(n-1)\phi_1(k_f-k_{s1})}{k_{s1}+(n-1)k_f+\phi_1(k_f-k_{s1})}$	$\frac{k_{nf}}{k_f} = \frac{k_s+(n-1)k_f-(n-1)\phi(k_f-k_s)}{k_s+(n-1)k_f+\phi(k_f-k_s)}$
Heat capacity	$(\rho C_p)_{hnf} = \left(\begin{array}{r} \left[(1-\phi_2)\left((1-\phi_1)(\rho C_p)_f+\phi_1(\rho C_p)_{s1}\right)\right] \\ +\phi_2(\rho C_p)_{s2} \end{array} \right)$	$(\rho C_p)_{nf} = (1-\phi)(\rho C_p)_f+\phi(\rho C_p)_s$
Density	$\rho_{hnf} = \left(\begin{array}{r} \left[(1-\phi_2)\left((1-\phi_1)(\rho C_p)_f+\phi_1(\rho C_p)_{s1}\right)\right] \\ +\phi_2(\rho C_p)_{s2} \end{array} \right)$	$\rho_{nf} = (1-\phi)\rho_f + \phi\rho_s$
Viscosity	$\mu_{hnf} = \frac{\mu_f}{(1-\phi_1)^{2.5}(1-\phi_2)^{2.5}}$	$\mu_{nf} = \frac{\mu_f}{(1-\phi)^{2.5}}$

See Uma Devi and Anali Devi (2017) and Manjunatha et al. (2019)

Friction factor coefficient (C_f) and reduced Nusselt number (Nu_x) are identified as: [following Uma Devi and Anali Devi (2017) and Manjunatha et al. (2019)]

$$C_f = \frac{\mu_{hnf}}{\rho_f u_w^2}\left(\frac{\partial u_1}{\partial y_1}\right)_{y_1=0} \tag{14}$$

$$C_f(\mathrm{Re}_x)^{\frac{1}{2}} = \frac{1}{\left((1-\phi_1)^{(2.5)}.(1-\phi_2)^{(2.5)}\right)}\frac{d^2f(0)}{d\zeta^2} \tag{15}$$

$$Nu_x = \frac{x_1 k_{hnf}}{k_f(T_f - T_\infty)}\left(\frac{\partial T}{\partial y_1}\right)_{y_1=0} \tag{16}$$

$$Nu_x(\mathrm{Re}_x)^{\left(\frac{-1}{2}\right)} = (-)\left(\frac{k_{hnf}}{k_f}+\frac{4}{3}R\right)\frac{d\theta(0)}{d\zeta} \tag{17}$$

$\mathrm{Re}_x = {u_w x_1}/{\upsilon_f}$ is the Reynolds number.

4 Calculation

The Runge–Kutta based shooting method is utilized with the MATLAB package to solve the nonlinear dimensionless Eqs. (11)–(13). For numerical computation we have considered values of the non-dimensionless parameter as $M = 0.5, R = 0.2, Bi = 0.2, \phi_1 = \phi_2 = 0.1, n = 3, \mathrm{Pr} = 6.2$. Here ϕ_1 is solid volume fraction of Graphene nanoparticles and ϕ_2 is aluminium oxide Al_2O_3 nanoparticles and $n = 3$ denotes shape of nanoparticles is spherical. For computation thermo physical properties of nanofluid and Hybrid nanofluid are applied from Table 1. Thermophysical properties of Graphene, aluminium oxide (Al_2O_3) and water at 25 °C are considered and listed in Table 2 Substantiation of Numerical code is tested via comparing the results incorporated in Table 3. The attained outcomes are in excellent concurrence with the published results of Uma Devi and Anali Devi (2017) and Manjunatha et al. (2019).

Table 2 Thermophysical properties of nanoparticles and water at 25 °C

Properties	Water (H_2O)	Graphene	Al_2O_3
Thermal conductivity $k\left(\frac{\mathrm{W}}{\mathrm{mK}}\right)$	0.6071	2500	40
Heat capacitance $C_p\left(\frac{\mathrm{J}}{\mathrm{kg\,K}}\right)$	4180	2100	765
Density $\rho\left(\frac{\mathrm{kg}}{\mathrm{m}^3}\right)$	997.0	2250	3970

See Uma Devi and Anali Devi (2017)

Numerical values for $C_f(\mathrm{Re}_x)^{\frac{1}{2}}$ and $Nu_x(\mathrm{Re}_x)^{\left(\frac{-1}{2}\right)}$ for various parameters for hybrid nanofluid (Graphene + aluminium oxide (Al_2O_3)/water)and Newtonian fluid are compared in Table 4. Numerical values for skin-friction coefficient $C_f(\mathrm{Re}_x)^{\frac{1}{2}}$ and Nusselt number $Nu_x(\mathrm{Re}_x)^{\left(\frac{-1}{2}\right)}$ for various parameters for regular nanofluid (Graphene + water, aluminium oxide $(Al_2O_3) + H_2O$) and hybrid nanofluid (Graphene + aluminium oxide (Al_2O_3)/water)are compared in Tables 5 and 6. Characteristics of assorted physical variables on the velocities $f'(\zeta)$ and temperature $\theta(\zeta)$ addressed in Figs. 2, 3, 4, 5, 6, 7 and 8 for various cases. In Figs. 2, 3 and 4 $f'(\zeta)$ and $\theta(\zeta)$ profiles are compared for Newtonian fluid $(\phi_1 = \phi_2 = 0)$ and hybrid nanofluid(Graphene + aluminium oxide (Al_2O_3) + water)case. Through Figs. 5, 6, 7 and 8 $f'(\zeta)$ and $\theta(\zeta)$ profiles are compared for nanofluid (Graphene + water, aluminium oxide (Al_2O_3) + H_2O)and hybrid nanofluid (Graphene + aluminium oxide (Al_2O_3)/water)case.

5 Results and discussion

The flawless perception of the theoretical flow problem is discussed in detail in this section. Figure 2 disclose the impact of increment in radiation parameter (R) on temperature $\theta(\zeta)$ profiles. It is evident that temperature

Table 3 Various values of Pr for the corresponding temperature gradient $\left(-\frac{d\theta(0)}{d\zeta}\right)$ when $Bi = B = M = \lambda = \phi_1 = \phi_2 = 0$

Pr	Uma Devi and Anali Devi (2017)	Manjunatha et al. (2019)	Present study
20.0	1.35390	1.35390	1.35390
7.0	1.89540	1.89540	1.89540
6.13	1.75968	1.75968	1.75968
2.0	0.91135	0.91135	0.91135

Table 4 Numerical values for $C_f(\mathrm{Re}_x)^{\frac{1}{2}}$ and $Nu_x(\mathrm{Re}_x)^{\left(\frac{-1}{2}\right)}$ for various parameters

R	M	Bi	$C_f(\mathrm{Re}_x)^{\frac{1}{2}}$		$Nu_x(\mathrm{Re}_x)^{\left(\frac{-1}{2}\right)}$	
			$\phi_1 = \phi_2 = 0$	$Al_2O_3 + H_2O +$ Graphene	$\phi_1 = \phi_2 = 0$	$Al_2O_3 + H_2O +$ Graphene
0.1			− 1.329577	− 2.199706	5.266084	2.986227
0.5			− 1.329577	− 2.199706	5.531590	3.107206
0.9			− 1.329576	− 2.199706	5.681491	3.175446
	0.1		− 1.156251	− 4.641766	− 1.899428	− 2.705365
	0.5		− 1.329577	− 4.640547	− 2.199706	− 2.704953
	0.9		− 1.482265	− 4.639482	− 2.462934	− 2.704595
		0.1	− 1.329577	− 2.199705	10.359453	5.895588
		0.3	− 1.329576	− 2.199706	3.692787	2.073125
		0.5	− 1.329577	− 2.199706	2.359453	1.308633

Table 5 Numerical values for skin-friction coefficient $C_f(\mathrm{Re}_x)^{\frac{1}{2}}$ for various parameters

M	R	Bi	n	Graphene + water	$Al_2O_3 + H_2O +$ Graphene	$Al_2O_3 + H_2O$
0				− 1.719525	− 2.256614	− 1.959539
1				− 2.488795	− 3.252657	− 2.669083
2				− 3.066905	− 4.002825	− 3.220435
	0.2			− 2.139089	− 2.799446	− 2.342092
	0.6			− 2.139089	− 2.799446	− 2.342092
	1			− 2.139089	− 2.799446	− 2.342092
		0.2		− 2.139089	− 2.799446	− 2.342092
		0.6		− 2.139089	− 2.799446	− 2.342092
		1		− 2.139089	− 2.799446	− 2.342092
			3	− 2.139089	− 2.799446	− 2.342092
			6	− 2.139089	− 2.799446	− 2.342092

distribution of the hybrid nanofluid and Newtonian fluid increases with increment in R. Physically, this is due to the increment in R produce more kinetic energy to the system. However, it is evident that Newtonian fluid shows higher $\theta(\zeta)$ profiles compared to hybrid nanofluid (Graphene + aluminium oxide (Al_2O_3) + water) thus for better cooling performance one can adopt this kind of hybrid nanofluid.

In Fig. 3 it is evident that, elevating values of magnetic parameter (M) depreciates velocity $f'(\zeta)$ of both Newtonian fluid and hybrid nanofluid (Graphene + aluminium oxide (Al_2O_3) + water). Here compare to hydromagnetic case hydrodynamic case is stronger. Lorentz force developed due to magnetic parameter become stronger with the increment in (M). Thus, stronger Lorentz force deteriorates the velocity $f'(\zeta)$.

In Fig. 4 it is observed that increment in Biot number (Bi) improves distribution of temperature in both Newtonian fluid and hybrid nanofluid $(Graphene + Al_2O_3 + H_2O)$. Since Biot number (Bi) includes the heat transfer coefficient h_i, this enhances for higher values of Bi.Therefore temperature augments. For $Bi = 0$ there is no heat transfer at the wall (insulated wall) as $Bi \to \infty$ one can obtain the prescribed surface temperature.

It is evident that Newtonian fluid demonstrates higher $\theta(\zeta)$ profiles compared to hybrid nanofluid $(Graphene +$

Table 6 Numerical values for Nusselt number $Nu_x(\mathrm{Re}_x)^{\left(\frac{-1}{2}\right)}$ for various parameters

M	R	Bi	n	Graphene + water	$Al_2O_3 + H_2O$ + Graphene	$Al_2O_3 + H_2O$
0				2.921934	2.250658	3.260554
1				2.922889	2.251224	3.261640
2				2.923592	2.251642	3.262466
	0.2			2.922457	2.250968	3.261142
	0.6			3.015356	2.315808	3.369747
	1			3.074921	2.357401	3.439545
		0.2		2.922457	2.250968	3.261142
		0.6		1.076705	0.821369	1.206835
		1		0.707554	0.535450	0.795973
			3	2.922457	2.250968	3.261142
			6	2.031612	1.281554	2.359910

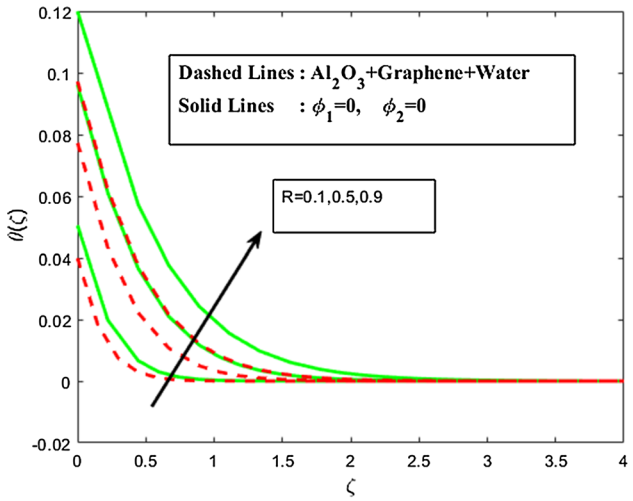

Fig. 2 Influence of radiation (R) on temperature $(\theta(\zeta))$

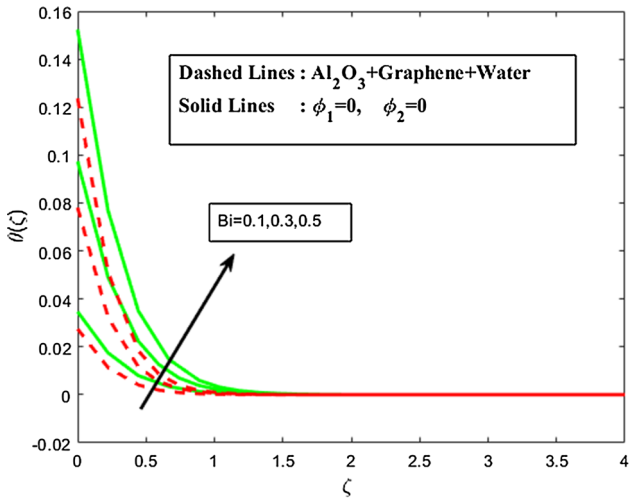

Fig. 4 Influence of Biot number (Bi) on temperature $(\theta(\zeta))$

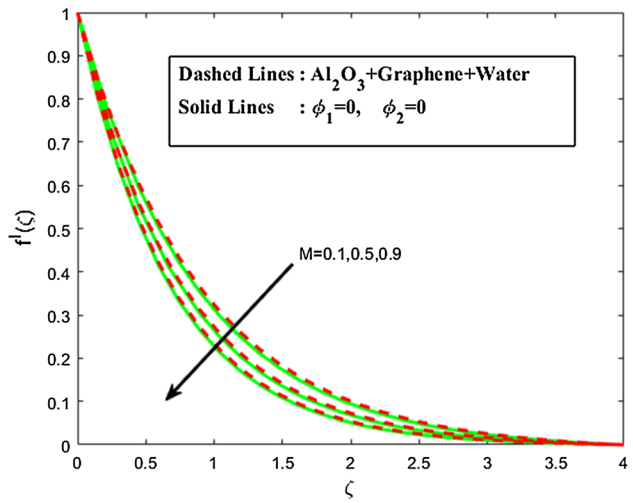

Fig. 3 Influence of magnetic parameter (M) on velocity $(f'(\zeta))$

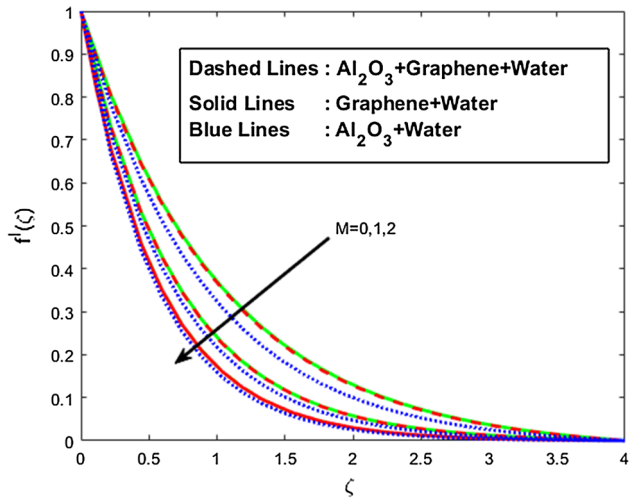

Fig. 5 Influence of magnetic parameter (M) on velocity $(f'(\zeta))$

$Al_2O_3 + H_2O$) thus for better cooling performance one can adopt this kind of hybrid nanofluid.

Through Fig. 5 the influence on velocity $f'(\zeta)$ profiles against the variation of magnetic parameter (M) is

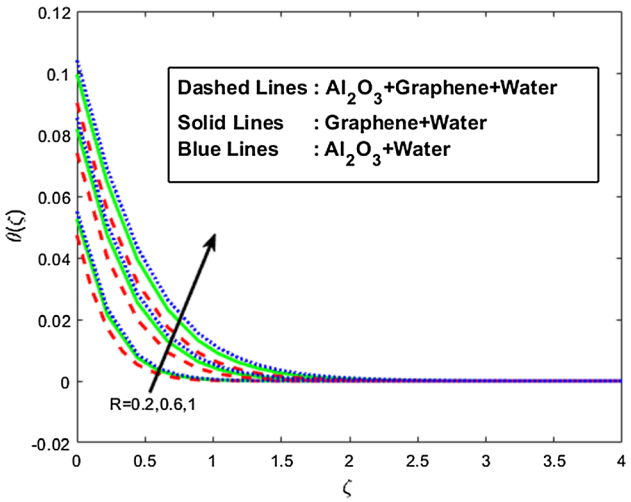

Fig. 6 Influence of radiation (R) on temperature $(\theta(\zeta))$

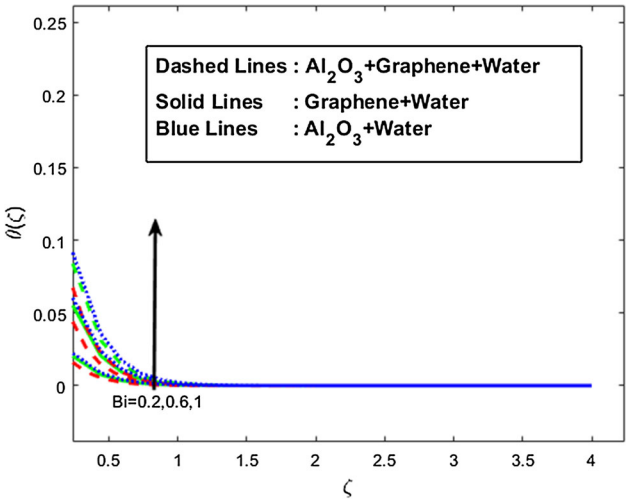

Fig. 7 Influence of Biot number (Bi) on temperature $(\theta(\zeta))$

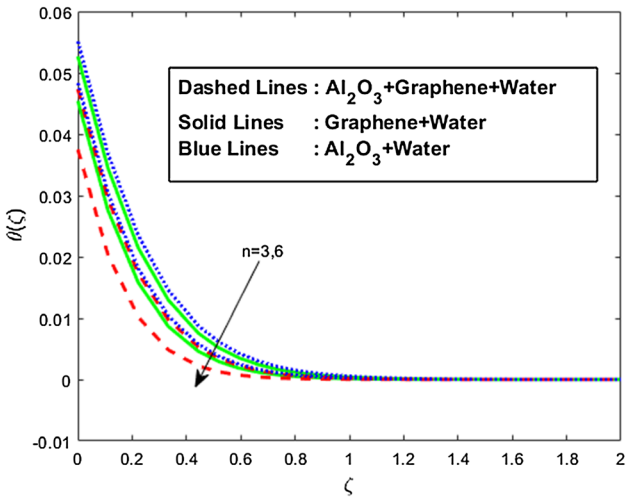

Fig. 8 Influence of shape of nanoparticles (n) on temperature $\theta(\zeta)$

portrayed for nanofluid Graphene/water $(Graphene+H_2O)$, aluminium oxide $(Al_2O_3)/H_2O$ $(Al_2O_3+H_2O)$ and hybrid nanofluid $(Graphene+Al_2O_3+H_2O)$. Improvement in M develops the Lorentz force thus $f'(\zeta)$ profile is decreased. It is observed that nanofluid shows lower $f'(\zeta)$ profiles compared to hybrid nanofluid $(Graphene+Al_2O_3+H_2O)$. Further $Al_2O_3+H_2O$ based nanofluid shows lower velocity profile compared to $Graphene+H_2O$ and $Graphene+Al_2O_3+H_2O$. This may be because of larger surface area provided by the $Graphene+Al_2O_3+H_2O$ and both graphene and aluminium nanoparticles are lighter in nature. In Fig. 6 influence of improving values of R on temperature $\theta(\zeta)$ is portrayed. Radiation improves the temperature distribution of the nanofluid $(Graphene+H_2O, Al_2O_3+H_2O)$, and hybrid nanofluid $(Graphene+Al_2O_3+H_2O)$. However, hybrid nanofluid $(Graphene+Al_2O_3+H_2O)$ shows lower temperature distribution compared to $Graphene+H_2O$ and $Al_2O_3+H_2O$ nanofluid. It is evident that $Al_2O_3+H_2O$ nanofluid shows higher temperature distribution. Thus hybrid nanofluid $(Graphene+Al_2O_3+H_2O)$ can be adopted for better cooling performance. In Fig. 7 Improvement in Biot number (Bi) improves temperature profile of the nanofluid $(Graphene+H_2O, Al_2O_3+H_2O)$, and hybrid nanofluid $(Graphene+Al_2O_3+H_2O)$. In Fig. 8 improvement in spherical size of the nanoparticles decrease the temperature profile in both nanofluid case and hybrid nanofluid case. Further it is witnessed that hybrid nanofluid $(Graphene+Al_2O_3+H_2O)$ case shows lower temperature distribution compared to nanofluid $(Graphene+H_2O, Al_2O_3+H_2O)$.Nanofluid $(Al_2O_3+H_2O)$ shows higher temperature distribution compared to other two cases. Thus, nanofluid $(Al_2O_3+H_2O)$ enhances thermal conductivity of the fluid. Hybrid nanofluid $(Graphene+Al_2O_3+H_2O)$ can be opted for cooling purpose.

From Table 3 it is evident that augmentation in Prandtl number (Pr) improves heat transfer rate of the Newtonian fluid but larger (Pr) diminishes heat transfer rate. This is because larger Prandtl number corresponds to weaker thermal diffusion.

From Table 4. It is noticed that, hybrid nanofluid $(Graphene+Al_2O_3+H_2O)$ shows lower friction rate and heat transfer rate compared to Newtonian fluid with the improvement in radiation (R), magnetic (M) and Biot number (Bi). From Table 5 it is witnessed that improving values of M lowers friction rate in nanofluid $(Graphene+H_2O, Al_2O_3+H_2O)$ and hybrid nanofluid $(Graphene+Al_2O_3+H_2O)$. Further, nanofluid (Graphene + water) shows higher friction rate compared to $(Al_2O_3+H_2O)$ and hybrid nanofluid $(Graphene+Al_2O_3+H_2O)$. From Table 6 it is observed that, rising values of magnetic parameter (M) improves the heat transfer rate in nanofluid $(Graphene+H_2O, Al_2O_3+H_2O)$ and hybrid

nanofluid $(Graphene + Al_2O_3 + H_2O)$. Further, Hybrid nanofluid shows lower heat transfer rate compared to nanofluid $(Graphene + H_2O, Al_2O_3 + H_2O)$. It is also witnessed that nanofluid $Al_2O_3 + H_2O$ shows higher heat transfer compared to Graphene + water. Improvement in R increases the heat transfer rate in nanofluid $(Graphene + H_2O, Al_2O_3 + H_2O)$ and hybrid nanofluid $(Graphene + Al_2O_3 + H_2O)$. Hybrid nanofluid shows lower heat transfer rate compared to nanofluid. Further, it is evident that nanofluid $Al_2O_3 + H_2O$ shows higher heat transfer compared to Graphene + water.

Larger values of Biot number (Bi) and shape of spherical nanoparticle (n) decreases the heat transfer rate in nanofluid $(Graphene + H_2O, Al_2O_3 + H_2O)$ hybrid nanofluid $(Graphene + Al_2O_3 + H_2O)$.

The results infer that usage of nanofluid $(Al_2O_3 + H_2O)$ significantly enhance convection heat transfer performance over a stretching sheet.

6 Conclusions

The impact of flow and heat transport of MHD, radiative Newtonian fluid, nanofluid $(Graphene + H_2O, Al_2O_3 + H_2O)$ and hybrid nanofluid $(Graphene + Al_2O_3 + H_2O)$ over a stretching sheet considering convective boundary condition is analyzed in this study through graphs and tables. The most noteworthy results are as follows.

- Obtained results indicate that the rate of heat transfer values for various mixture as Graphene + water (2.921934), Al_2O_3 + H_2O + Graphene (2.250658) and $Al_2O_3 + H_2O$ (3.260554). Thus, water based Al_2O_3 + graphene hybrid nanofluid can be opted for cooling performance.
- The friction at the wall for Graphene + water (− 1.719525), $Al_2O_3 + H_2O$ + Graphene (− 2.256614) and $Al_2O_3 + H_2O$ (− 1.959539). Thus, water based Al_2O_3 + graphene hybrid nanofluid shows lower wall friction rate.
- Newtonian fluid shows higher temperature distribution compared to hybrid nanofluid $(Graphene + Al_2O_3 + H_2O)$.
- Hybrid nanofluid $(Al_2O_3 + H_2O$ + Graphene) shows lower wall friction rate compared to nanofluid $(Graphene + H_2O, Al_2O_3 + H_2O)$.
- Graphene/water nanofluid shows higher wall friction compared to Al_2O_3/water nanofluid.
- Hybrid nanofluid $(Graphene + Al_2O_3 + H_2O)$ shows lower heat transfer rate compared to nanofluid $(Graphene + H_2O, Al_2O_3 + H_2O)$.
- Nanofluid $(Al_2O_3 + H_2O)$ significantly enhance convection heat transfer performance over a stretching sheet.

References

Abd El-Aziz M, Afify AA (2019) MHD Casson fluid flow over a stretching sheet with entropy generation analysis and Hall influence. Entropy 21(6):592

Abdelrazek AH, Kazi SN, Alawi OA, Yusoff N, Oon CS, Ali HM (2020) Heat transfer and pressure drop investigation through pipe with different shapes using different types of nanofluids. J Therm Anal Calorim 139(3):1637–1653

Babar H, Sajid MU, Ali HM (2019) Viscosity of hybrid nanofluids: a critical review. Therm Sci 23(3 Part B):1713–1754

Chen A, Lin TF, Ali HM, Yan WM (2020) Experimental study on bubble characteristics of time periodic subcooled flow boiling in annular ducts due to wall heat flux oscillation. Int J Heat Mass Transf 2020(157):119974

Goodarzi M, Tlili I, Tian Z, Safaei MR (2019) Efficiency assessment of using graphenenanoplatelets-silver/water nanofluids in microchannel heat sinks with different cross-sections for electronics cooling. Int J Numer Methods Heat Fluid Flow 30(1):347–372

Gopal D, Naik SH, Kishan N, Raju CS (2020) The impact of thermal stratification and heat generation/absorption on MHD Carreau-nano fluid flow over a permeable cylinder. SN Appl Sci 2(4):1

Hayat T, Aziz A, Muhammad T, Alsaedi A (2019) Numerical simulation for Darcy–Forchheimer three-dimensional rotating flow of nanofluid with prescribed heat and mass flux conditions. J Therm Anal Calorim 136(5):2087–2095

Khalid SU, Babar H, Ali HM, Janjua MM, Ali MA (2020) Heat pipes: progress in thermal performance enhancement for microelectronics. J Therm Anal Calorim. https://doi.org/10.1007/s10973-020-09820-7

Kumar R, Raju CS, Sekhar KR, Reddy GV (2019) Three dimensional MHD ferrous nanofluid flow over a sheet of variable thickness in slip flow regime. J Mech 35(2):255–266

Kumar KG, Lokesh HJ, Shehzad SA, Ambreen T (2020a) On analysis of Blasius and Rayleigh–Stokes hybrid nanofluid flow under aligned magnetic field. J Therm Anal Calorim 139(3):2119–2127

Kumar KA, Sugunamma V, Sandeep N (2020b) Influence of viscous dissipation on MHD flow of micropolar fluid over a slendering stretching surface with modified heat flux model. J Therm Anal Calorim 139(6):3661–3674

Manjunatha S, Kuttan BA, Jayanthi S, Chamkha A, Gireesha BJ (2019) Heat transfer enhancement in the boundary layer flow of hybrid nanofluids due to variable viscosity and natural convection. Heliyon 5(4):e01469

Muhammad K, Hayat T, Alsaedi A, Ahmad B (2020) Melting heat transfer in squeezing flow of basefluid (water), nanofluid (CNTs + water) and hybrid nanofluid (CNTs + CuO + water). J Therm Anal Calorim 19:1–8

Raju CS, Mamatha SU, Rajadurai P, Khan I (2019a) Nonlinear mixed thermal convective flow over a rotating disk in suspension of magnesium oxide nanoparticles with water and EG. Eur Phys J Plus 134(5):196

Raju CS, Saleem S, Al-Qarni MM, Upadhya SM (2019b) Unsteady nonlinear convection on Eyring-Powell radiated flow with suspended graphene and dust particles. Microsyst Technol 25(4):1321–1331

Raju CS, Sandeep N, Ali ME, Nuhait AO (2019c) Heat and mass transfer in 3-D MHD Williamson–Casson fluids flow over a stretching surface with non-uniform heat source/sink. Therm Sci 23(1):281–293

Sajid MU, Ali HM (2018) Thermal conductivity of hybrid nanofluids: a critical review. Int J Heat Mass Transf 126:211–234

Sajid MU, Ali HM (2019) Recent advances in application of nanofluids in heat transfer devices: a critical review. Renew Sustain Energy Rev 103:556–592

Sajid MU, Ali HM, Sufyan A, Rashid D, Zahid SU, Rehman WU (2019) Experimental investigation of TiO_2–water nanofluid flow and heat transfer inside wavy mini-channel heat sinks. J Therm Anal Calorim 137(4):1279–1294

Sarafraz MM, Safaei MR (2019) Diurnal thermal evaluation of an evacuated tube solar collector (ETSC) charged with graphene-nanoplatelets-methanol nano-suspension. Renew Energy 142:364–372

Sarafraz MM, Safaei MR, Tian Z, Goodarzi M, BandarraFilho EP, Arjomandi M (2019) Thermal assessment of nano-particulate graphene-water/ethylene glycol (WEG 60: 40) nano-suspension in a compact heat exchanger. Energies 12(10):1929

Seth D, Shrivastava RL, Shrivastava S (2016) An empirical investigation of critical success factors and performance measures for green manufacturing in cement industry. J Manuf Technol Manag 27(8):1076–1101

Seth D, Rehman MAA, Shrivastava RL (2018) Green manufacturing drivers and their relationships for small and medium (SME) and large industries. J Clean Prod 198:1381–1405

Shahsavar A, Ali HM, Mahani RB, Talebizadehsardari P (2020) Numerical study of melting and solidification in a wavy double-pipe latent heat thermal energy storage system. J Therm Anal Calorim. https://doi.org/10.1007/s10973-020-09864-9

Sheikholeslami M, Gerdroodbary MB, Shafee A, Tlili I (2019) Hybrid nanoparticles dispersion into water inside a porous wavy tank involving magnetic force. J Therm Anal Calorim. https://doi.org/10.1007/s10973-019-08858-6

Sriharan G, Harikrishnan S, Ali HM (2020) Experimental investigation on the effectiveness of MHTHS using different metal oxide based nanofluids. J Therm Anal Calorim. https://doi.org/10.1007/s10973-020-09779-5

Tariq HA, Anwar M, Malik A, Ali HM (2020) Hydro-thermal performance of normal-channel facile heat sink using TiO_2–H_2O mixture (Rutile-Anatase) nanofluids for microprocessor cooling. J Therm Anal Calorim. https://doi.org/10.1007/s10973-020-09838-x

Uma Devi S, Anali Devi SP (2017) Heat transfer enhancement of Cu–Al_2O_3/water hybrid nanofluid flow over a stretching sheet. Niger Math Soc 36:419–433

Upadhya SM, Devi RLVR, Raju CSK et al (2020) Magnetohydrodynamic nonlinear thermal convection nanofluid flow over a radiated porous rotating disk with internal heating. J Therm Anal Calorim. https://doi.org/10.1007/s10973-020-09669-w

Wakif A, Chamkha A, Thumma T, Animasaun IL, Sehaqui R (2020) Thermal radiation and surface roughness effects on the thermo-magnetohydrodynamic stability of alumina–copper oxide hybrid nanofluids utilizing the generalized Buongiorno's nanofluid model. J Therm Anal Calorim. https://doi.org/10.1007/s10973-020-09488-z